Inorganica Chimica Acta 362 (2009) 1935–1942

Contents lists available at ScienceDirect

Inorganica Chimica Acta

journal homepage: www.elsevier.com/locate/ica

Synthesis and structural characterization of new chiral mixed phosphine phosphoramidite complexes of ruthenium

Stephen Costin, Nigam P. Rath, Eike B. Bauer *

University of Missouri – St. Louis, Department of Chemistry and Biochemistry, One University Boulevard, St. Louis, MO 63121, USA

ARTICLE INFO

Article history:
Received 16 July 2008
Received in revised form 2 September 2008
Accepted 4 September 2008
Available online 11 September 2008

Keywords:
Ruthenium
Phosphoramidites
Cyclic voltammetry
X-ray
Chiral at metal
Mukaiyama aldol reaction

ABSTRACT

New phosphoramidite complexes of ruthenium chiral at the metal were synthesized, structurally characterized and their electrochemical and catalytic properties were studied. Reaction of the known chiral phosphoramidites $(RO)_2PNR'_2$ (R = naphthyl, R′ = CH_3, **1a**; R = naphthyl, R′ = benzyl, **1b**; R = octahydronaphthyl, R′ = benzyl, **1c**) with $CpRu(PPh_3)_2Cl$ afforded the title compounds $CpRu(PPh_3)$(**1a–c**)(Cl) (**2a–c**) in 46–74% isolated yields. Fractional crystallization of **2b** and **2c** afforded the corresponding diastereopure complexes which are chiral both at the metal and at the ligand. The molecular structures of **2b** and **2c** were determined, revealing a pseudo octahedral coordination geometry about the ruthenium center. Electrochemical studies by cyclic voltammetry showed reversible electrochemical behavior of the metal complexes **2a–c**. The new metal complexes are catalytically active in the Mukaiyama aldol reaction (24 h, room temperature, 31–53% yield), but almost no enantiomeric excesses for the products were obtained.

1. Introduction

Phosphoramidites are a monodentate, P-coordinating ligand class, featuring two oxygen atoms and one nitrogen atom bonded to the phosphorus center (Fig. 1) [1]. Originally described by Feringa [1b], they are increasingly applied as ligands in transition metal catalyzed organic transformations such as enantioselective conjugate enone addition reactions [1f,2], hydrogenations [1a,1c,3], allylic alkylations [4], hydrosilylations [5], vinylations [6], cycloadditions [7], Diels–Alder [8] and Heck reactions [9]. Due to secondary interactions of aromatic ring systems on the ligand with the metal center, phosphoramidites can serve as two-, four-, six- or eight-electron donors [10].

It is known that phosphoramidite ligands (L) form ruthenium complexes with the general formula (*p*-cymene)Ru(L)$(Cl)_2$ [11]. The *p*-cymene ligand detaches from these metal complexes at elevated temperatures, potentially opening decomposition pathways.

We were looking for a more robust platform for piano stool type phosphoramidite complexes of ruthenium and assumed that replacing the *p*-cymene ligand with a cyclopentadienyl (Cp) ligand would give rise to more stable architectures. We also were interested in synthesizing phosphoramidite complexes that are chiral at the metal. Herein we describe the synthesis and structural characterization of ruthenium phosphoramidite complexes with the general formula $CpRu(PPh_3)(L)(Cl)$. These complexes are the first Cp phosphoramidite complexes of ruthenium and they are chiral at the metal. We investigated the electrochemistry of the new complexes and applied them as catalysts in the Mukaiyama aldol reaction.

2. Results and discussion

To achieve our objectives, commercial $CpRu(PPh_3)_2Cl$ seemed to be a suitable precursor. This complex is known to give half-sandwich complexes of the type $CpRu(PPh_3)(L)(Cl)$ by PPh_3 exchange when treated with monodentate phosphines [12]. Accordingly, the known [13] ligand **1a** was reacted with an equimolar amount of $CpRu(PPh_3)_2Cl$ in $CHCl_3$ under reflux for 8 h, as shown in Scheme 1 (top reaction). Chromatographic workup of the reaction mixture provided the new chiral target complex $CpRu(PPh_3)$(**1a**)(Cl) (**2a**) as a 5:3 mixture of diastereomers (assessed by ^1H NMR). Efforts to separate the stereoisomers and to obtain diastereomerically pure material have failed so far. We speculated that the relatively small methyl groups on nitrogen create only slight steric congestion at the metal, rendering the two diastereomers close in energy. Thus, the known ligand **1b** [13] featuring two bulkier benzyl groups on nitrogen was next employed in complex synthesis. Under the standard conditions described above (but with 16 h reaction time), ligand **1b** gave an 8:1 mixture of diastereomers (^1H NMR) of complex **2b** after flash chromatography. It was possible to isolate the major diastereomer by fractional crystallization from CH_2Cl_2/MeOH to obtain diastereopure **2b** in 74% yield.

To investigate if changes in the naphthyl backbone have an influence on the properties of the corresponding metal complex,

* Corresponding author.
E-mail address: bauere@umsl.edu (E.B. Bauer).

0020-1693/$ - see front matter © 2008 Elsevier B.V. All rights reserved.
doi:10.1016/j.ica.2008.09.003

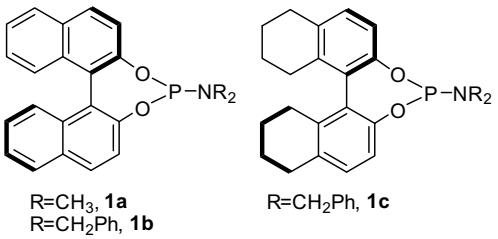

Fig. 1. Phosphoramidite ligands.

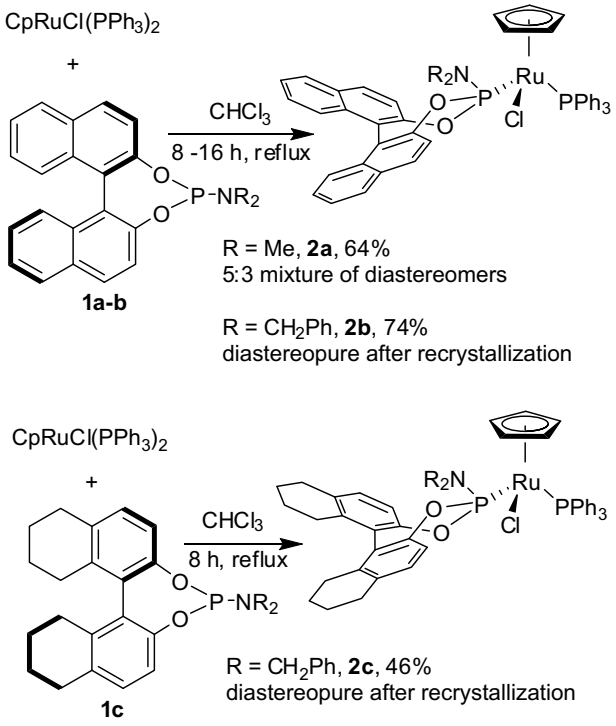

Scheme 1. Phosphoramidite complex syntheses.

the ligand **1c** was synthesized following a literature procedure [14]. Phosphoramidite ligand **1c** was converted to its ruthenium complex **2c** as described above for **2b** (Scheme 1, bottom). After flash chromatography, an 8:1 mixture of diastereomers was obtained (^{1}H NMR), and the major diastereomer was isolated by fractional crystallization from CH_2Cl_2/MeOH to obtain **2c** diastereopure in 46% yield.

All new mixed phosphoramidite PPh_3 ruthenium complexes **2a–c** were obtained as orange powders and characterized by NMR (^{1}H, ^{13}C, ^{31}P), mass spectrometry, IR, and microanalysis.

In the ^{31}P NMR, two doublets were observed for the phosphoramidite and the PPh_3 ligands. The coordination of the phosphoramidite ligand was best observed by a downfield shift of the phosphorus signal. The free ligands have chemical shifts between 140 and 150 ppm, whereas the ruthenium complexes **2a–c** exhibited signals for the coordinated phosphoramidite ligands between 163.8 and 177.8 ppm. The PPh_3 ligands showed signals between 45.2 and 48.0 ppm. The J_{PP} coupling constants for the two different phosphorus atoms in the metal complexes ranged from 148.5 to 168.0 Hz.

Due to the coordination of the phosphoramidite ligand to the ruthenium center, all aromatic ring atoms become diastereotopic, and give in principle different ^{13}C NMR signals for each carbon atom (but the peaks are in practice not always resolved). Some of the aromatic carbon atoms couple with the phosphorus atoms (J_{CP} = 12–60 Hz). As a consequence, a complex ^{13}C NMR spectrum appears in the aromatic region. However, the number of signals did not reach the number of diastereotopic aromatic carbons, and some of the peaks were broad and some of them had shoulders (or other non-Gaussian features). Similarly, the four protons of the two NCH_2 groups in **2b** and **2c** are diastereotopic and gave four distinct signals in the ^{1}H NMR. The Cp ligands gave sharp singlets between 4.48 and 4.71 ppm.

The FAB mass spectra showed a strong molecular ion peak for the metal complexes, and a somewhat weaker peak arising from loss of Cl.

To unequivocally establish the structures of the new ruthenium phosphoramidite complexes, the crystal structures of the complexes **2b** and **2c** described above were determined (Table 1 and Section 4). The molecular structures are depicted in Fig. 2 and Table 2 shows key structural data.

In general, the two ruthenium complexes do not show large structural differences. Key bond lengths and angles are similar, as well as the distance between the ruthenium center and the Cp centroid (Table 2).

The bond angles around ruthenium range from 87.37(3)° for the Cl(1)–Ru–P(1) angle to 99.11(3)° for the P(1)–Ru–P(2) angle. Thus, the coordination geometry of the complexes is best described as octahedral with slight distortions and with the largest angles observed between PPh_3 and the bulky phosphoramidite ligands (99.11(3)° and 97.88(6)°, respectively).

The PPh_3 Ru–P(1) bond lengths for both complexes (2.3294(8) and 2.3231(16) Å) are slightly longer than the corresponding phosphoramidite Ru–P(2) bond lengths (2.2426(8) and 2.2404(14) Å). The stronger bond between the phosphorus atom of the phosphoramidite and the ruthenium center might be explained by stronger backbonding for this ligand.

For both ruthenium complexes **2b** and **2c**, the two phenyl rings connected to the phosphorus form an angle α (Fig. 3). It is larger for complex **2c** (59.74°) than for complex **2b** (49.51°) and is the biggest structural difference between the two complexes. In complex **2c,** half of each naphthyl ring is hydrogenated, and thus non-aromatic. Repulsive forces between the two non-planar rings might contribute to a larger angle α. In turn, the angle α has no influence on the O(1)–P(2)–O(2) angle, which is for both complexes almost identical (Table 2, entry 8).

Complexes **2b** and **2c** are chiral at the metal. According to the priority order C_5H_5 > Cl > P(2) > P(1) [15,16], the absolute configuration of these complexes is (R), as determined from the X-ray structures.

To obtain additional information for the new metal complexes, additional experiments were performed. We were interested in whether the new diastereopure ruthenium complexes are configurationally stable at elevated temperatures, which would have importance in their application in catalysis. Thus, an NMR sample of diastereopure **2b** in $CDCl_3$ was heated at 90 °C for 3 h and monitored by ^{31}P NMR (Scheme 2). The sample slowly decomposed over time, but no signals for the other diastereomer were observed in the ^{31}P NMR spectrum suggesting that complex **2b** is configurationally stable even at elevated temperatures.

We also were interested in whether both PPh_3 ligands could be substituted for phosphoramidite ligands. Thus, 2.5 equiv. of the phosphoramidite ligand **1b** were combined with one equivalent of $CpRu(PPh_3)_2Cl$ in $CDCl_3$ and heated at 90 °C for 24 h. The ^{31}P NMR spectra revealed that besides monosubstitution, some disubstitution took place. In addition to the two doublets for the monosubstituted product **2b**, two new doublets at 171.5 and 179.9 ppm were observed. These peaks are broad and of much lower intensity than the peaks for **2b**. The ^{31}P NMR also showed that unreacted **1b** still was present in the reaction mixture. A FAB mass spectrum

Table 1
Crystallographic parameters

	2b · $(THF)_2$	**2c** · $(CHCl_3)_2$
Empirical formula	$C_{65}H_{62}ClNO_4P_2Ru$	$C_{59}H_{56}Cl_7NO_2P_2Ru$
Formula weight	1119.62	1222.21
Temperature (K)/wavelength (Å)	100(2)/0.71073	100(2)/0.71073
Crystal system	monoclinic	orthorhombic
Space group	$P2_1$	$P2_12_12_1$
Unit cell dimensions		
a (Å)	11.036(2)	12.4499(9)
b (Å)	13.859(2)	15.5701(12)
c (Å)	17.620(3)	28.516(2)
α (°)	90	90
β (°)	99.349(8)	90
γ (°)	90	90
V (Å^3)/Z	2659.0(8)/2	5527.8(7)/4
D_{calc} (Mg/m^3)	1.398	1.621
Absorption coefficient (mm^{-1})	0.457	0.724
F(000)	1164	2504
Crystal size (mm^3)	0.28 × 0.23 × 0.21	0.24 × 0.22 × 0.20
Theta range for data collection (°)	2.94–27.00	2.62–26.47
Index ranges	$-14 \leqslant h \leqslant 14$, $-17 \leqslant k \leqslant 17$, $-22 \leqslant l \leqslant 22$	$-15 \leqslant h \leqslant 14$, $-19 \leqslant k \leqslant 19$, $35 \leqslant l \leqslant 35$
Reflections collected	72549	147736
Independent reflections	11479 [R(int) = 0.059]	11368 [R(int) = 0.071]
Absorption correction	semi-empirical from equivalents	semi-empirical from equivalents
Maximum and minimum transmission	0.9102 and 0.8812	0.8699 and 0.8006
Data/restraints/parameters	11479/1/697	11368/0/658
Goodness-of-fit on F^2	1.032	1.114
Final R indices [I > 2sigma(I)]	R_1 = 0.0326, wR_2 = 0.0708	R_1 = 0.0639, wR_2 = 0.1562
R indices (all data)	R_1 = 0.0373, wR_2 = 0.0731	R_1 = 0.0703, wR_2 = 0.1599
Largest difference in peak and hole (e Å^{-3})	0.663 and −0.484	1.793 and −1.622
Absolute structure parameter	−0.009(16)	0.03(4)

exhibited, in addition to a peak for **2b**, also a peak for the doubly substituted product. The NMR and MS data suggest that the second substitution occurs but it is a sluggish and incomplete process, potentially leading to a less stable product showing some dynamic behavior in solution. The bulky phosphoramidite ligands presumably create too much steric constraint about the ruthenium center resulting in an unstable material.

In order to obtain preliminary insight into the electronic properties of the new metal complexes, cyclic voltammograms of the phosphoramidite ligands **1a–c** and the metal complexes **2a–c** were recorded as described in Section 4. For comparison, a cyclic voltammogram of the ruthenium precursor $CpRu(PPh_3)_2Cl$ was recorded as well. Key data are listed in Table 3 and two representative traces for ligand **1a** and its ruthenium complex **2a** are depicted in Fig. 4. The traces for the other ligands and complexes are given in the Supplementary material.

The cyclic voltammograms of the phosphoramidite ligands suggest complex and irreversible chemical reactions taking place after oxidation [17]. Scans towards increasing positive potential show an irreversible oxidation wave without a reduction wave on the reverse scan. The potentials of the free phosphoramidite ligands for the first oxidation differed between 1.37 and 1.70 V (vs. ferrocene/ferrocenium). Thus, the oxidation potentials of the phosphoramidite ligands show a slight dependency on their substituents.

The cyclic voltammograms for the corresponding metal complexes **2a–c** show a fair degree of reversibility in that a reduction wave is seen for each complex that appears similar in size and is of complementary shape to the first oxidation wave. The $E_{1/2}$ values for the oxidation range from 0.56 to 0.63 V (vs. ferrocene/ferrocenium) and the peak current ratios i_c/i_a are $\geqslant$0.95 (Table 3). While the ideal separation between the oxidation and reduction peaks for a diffusing species undergoing a one electron oxidation–reduction cycle is 59 mV, the peak-to-peak separations ΔE seen here are between 0.23 and 0.41 V suggesting sluggish electron transfer. At higher potentials up to 2 V, no additional oxidation waves were observed.

Whereas the ligands alone show irreversible electrochemical behavior, the formation of the complex yields much greater signs of reversibility. This suggests that a one-electron oxidation and reduction is occurring that involves a highest occupied molecular orbital found only for the complex and not for the ligand alone. The precursor complex $CpRu(PPh_3)_2Cl$ has an $E_{1/2}$ value of 0.49 V, which is somewhat lower than those of the ruthenium phosphoramidite complexes **2a–c**. Strictly speaking, the E_a values for the free ligands and the $E_{1/2}$ values for the metal complexes cannot be compared. However, the potentials of the ligands seem to be generally higher than those of their respective metal complexes, suggesting a metal-centered HOMO.

Finally, we were interested to determine if the new complexes are suitable as catalysts in organic transformations. To maintain the stereochemical properties of the metal complexes, we targeted chloride abstraction as a suitable method for activation. It is known that reagents such as $TlPF_6$ and $(Et_3O)(PF_6)$ selectively remove chloride ligands from metal complexes [18]. If performed with our metal complexes, a chiral Lewis acid would be the result of the activation. Many organic transformations are catalyzed by Lewis acids, and we found the Mukaiyama aldol reaction especially appealing, as it allows for asymmetric carbon–carbon bond formation [19].

First, we tested if $(Et_3O)(PF_6)$ removes selectively the chloride from complex **2b**. An NMR tube experiment in $CDCl_3$ showed that combination of 1 equiv. of complex **2b** and $(Et_3O)(PF_6)$ resulted in spectra, which show no remaining starting material (^{1}H, ^{31}P). Three new broad signals showed up in the ^{31}P NMR spectrum (one singlet at 14.4 ppm and two doublets at 47.2 and 185.6 ppm, J_{PP} = 62 Hz), suggesting dynamic processes as a result of chloride abstraction. After removal of the solvent, a FAB mass spectrum of the residue no longer exhibited a molecular ion peak for **2b**, but a molecular ion peak for a compound of the general formula $[CpRu(PPh_3)(\mathbf{1b})]^+$, missing the chloride ligand was present (Scheme 2). Identical results were obtained when $AgPF_6$ in CH_2Cl_2 was employed as chloride scavenger. The chloride abstraction was sluggish and

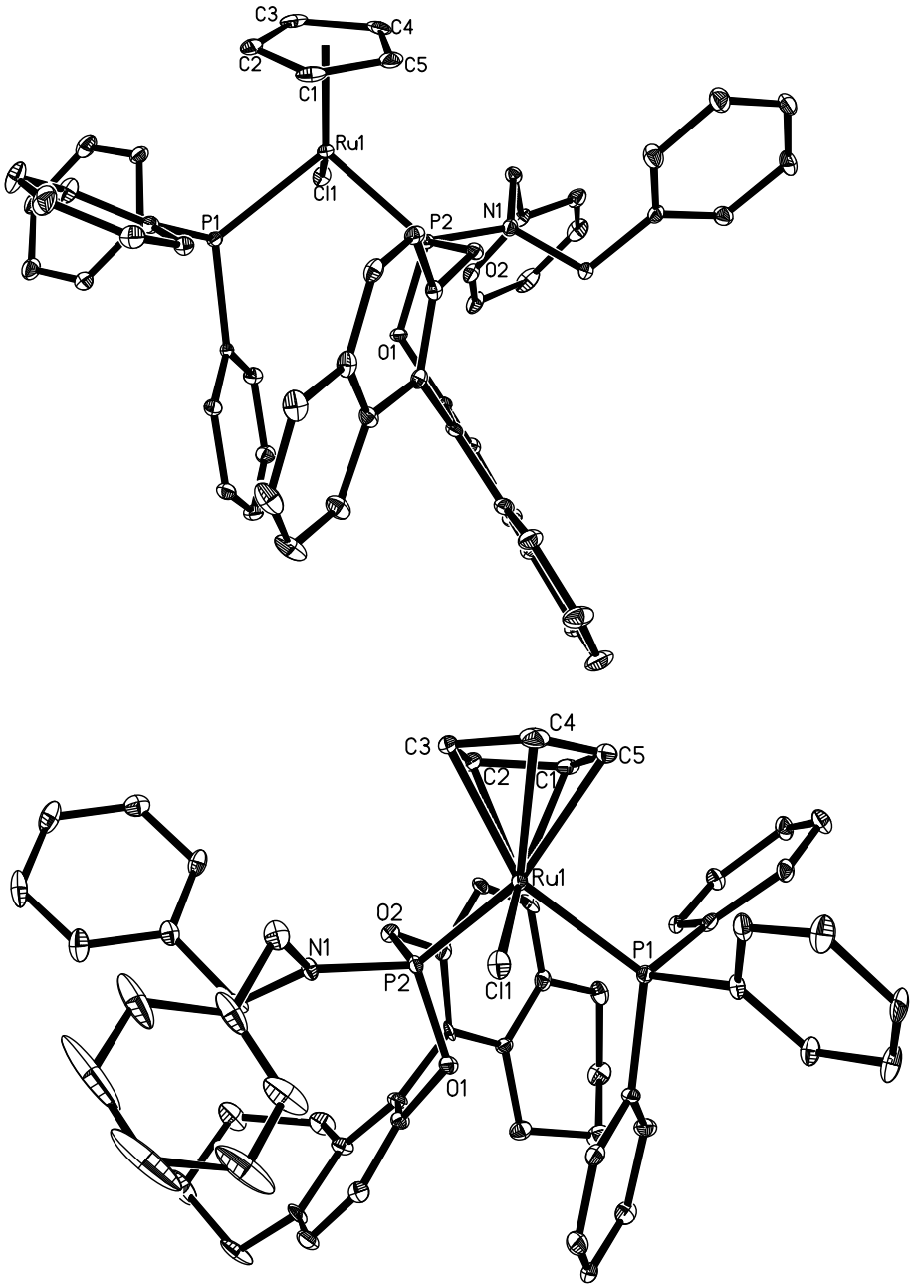

Fig. 2. Molecular structures of the ruthenium phosphoramidite complexes **2b** (top) and **2c** (bottom). Solvent molecules are omitted for clarity.

Table 2
Selected bond lengths, angles and calculated values for ruthenium phosphoramidite complexes

Entry	Complex	**2b** · $(THF)_2$	**2c** · $(CHCl_3)_2$
Bond lengths (Å)			
1	Ru–P(1)	2.3294(8)	2.3231(16)
2	Ru–P(2)	2.2426(8)	2.2404(14)
3	Ru–Cl(1)	2.4302(7)	2.4415(16)
4	P(2)–N(1)	1.653(3)	1.646(5)
Bond angles (°)			
5	Cl(1)–Ru–P(1)	87.37(3)	88.05(6)
6	Cl(1)–Ru–P(2)	92.28(3)	93.85(6)
7	P(1)–Ru–P(2)	99.11(3)	97.88(6)
8	O(1)–P(2)–O(2)	99.21(9)	99.5(2)
Calculated values (Mercury 1.4.2)			
9	Angle α (Fig. 3) (°)	49.51	59.74
10	Ru–Cp distance (Å)	1.850	1.850

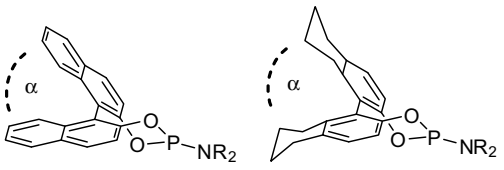

Fig. 3. Schematic representation of angle α.

incomplete when $TlPF_6$ was used, and does not work with $(Et_3O)(PF_6)$ in diethylether or THF, leaving the starting material **2b** unreacted. Due to its high reactivity, all efforts to isolate [CpRu(PPh_3)(**1b**)]PF_6 have failed to date.

Next, we tested if the activated metal complex is catalytically active in the Mukaiyama aldol reaction. A solution of the catalyst activated by $(Et_3O)(PF_6)$ was added to *tert*-butyl(1-methoxyvinyloxy)dimethylsilane (**3**) and the corresponding aromatic carbonyl

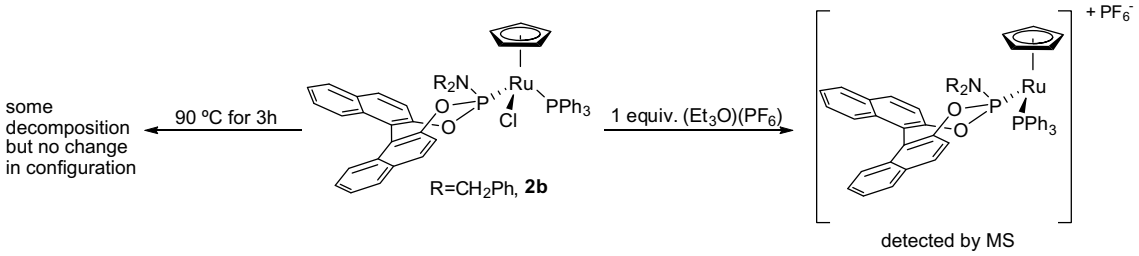

Scheme 2. Experiments to understand the reactivity of complex **2b**.

Table 3
Cyclic voltammetry data of ruthenium phosphoramidite complexes

Complex	$E_{1/2}$/V[a]	ΔE/V[a]	i_c/i_a[a]	E_{pa}/V[a]	E_{pa}/V[b] free ligand **1**
$CpRu(PPh_3)_2Cl$	0.49	0.23	0.95	0.61	
2a	0.56	0.23	1.0	0.76	1.37
2b	0.63	0.27	0.96	0.80	1.63
2c	0.56	0.41	1.0	0.76	1.70

[a] Referenced against ferrocene as internal standard (see Section 4).
[b] First oxidation potential.

compound **4**, and the sample was analyzed and worked up after 24 h at room temperature. The results are compiled in Table 4. A control experiment showed that $(Et_3O)(PF_6)$ also catalyzes the reaction at least of **4a** and **4b** with *tert*-butyl(1-methoxyvinyloxy)dimethylsilane (**3**). Thus, special care was taken when complex **2b** was activated; it was employed in slight excess to make sure that the activated metal complex did not contain residual $(Et_3O)(PF_6)$.

After 24 h at room temperature, the silane **3** was completely consumed, and some carbonyl starting material **4** was left over in the

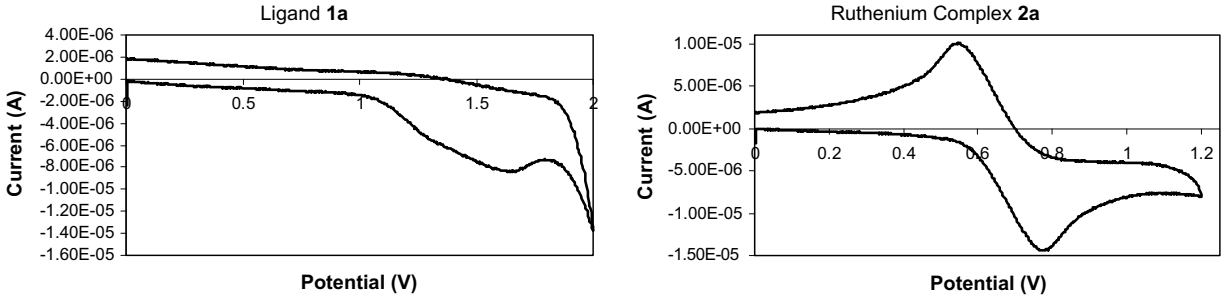

Fig. 4. Representative cyclic voltammograms for the free ligand **1a** and its ruthenium complex **2a** (before referencing to ferrocene/ferrocenium).

Table 4
Catalytic results of the Mukaiyama aldol reaction

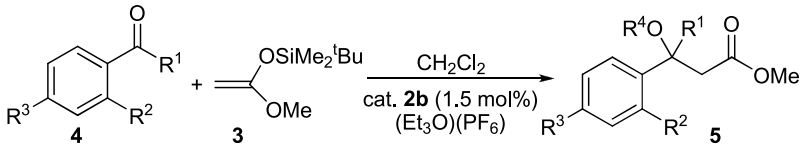

Entry[a]	Substrate	Product	Yield[b] (%)	ee (%)
1	$R^1 = R^2 = R^3 = H$ **4a**	$R^1 = R^2 = R^3 = H$, $R^4 = SiMe_2{}^tBu$, **5a**	53 (42)[d]	3[c]
2	$R^1 = CH_3$, $R^2 = R^3 = H$, **4b**	$R^1 = CH_3$, $R^2 = R^3 = H$, $R^4 = SiMe_2{}^tBu$, **5b**	48	5[e]
3	$R^1 = R^2 = H$, $R^3 = OMe$, **4c**	$R^1 = R^2 = H$, $R^3 = OMe$, $R^4 = SiMe_2{}^tBu$, **5c**	50	[f]
4	$R^1 = R^3 = H$, $R^2 = Cl$, **4d**	$R^1 = R^3 = H$, $R^2 = Cl$, $R^4 = H$, **5d**	31	2[c]

[a] Conditions: catalyst **2b** (0.007 mmol) was preactivated with $(Et_3O)(PF_6)$ in CH_2Cl_2 and after 2 h added to the substrates **3** and **4** (0.472 mmol each). The resulting solution was maintained at room temperature for 24 h.
[b] Isolated yield after chromatography.
[c] Determined by chiral GC.
[d] Isolated yield when the reaction was performed in the presence of 20 mol% 2,6-di-*tert*-butylpyridine.
[e] Determined by ^1H NMR with a chiral shift reagent.
[f] Determination of the enantiomeric excess was not possible.

reaction mixture, as determined by GC/MS. A strong product peak was observed. Chromatographic workup afforded the corresponding silyloxy esters (**5**) in 31–53% isolated yields (Table 4). However, as assessed by chiral GC or ^{1}H NMR with a chiral shift reagent, only small enantiomeric excesses for the products **5** were obtained.

The lack of enantioselectivity can be rationalized as follows. It might indeed be that the architecture of the metal complex after chloride abstraction does not allow for stereodifferentiation under the reaction conditions. It also might be that the fragment [CpRu(PPh_3)(**1b**)]$^+$ (Scheme 2) is configurationally not stable. On the other hand, it is known that besides Lewis acids, strong Brønsted acids catalyze the Mukaiyama aldol reaction [20]. Thus, another possibility is that the strong Lewis acid resulting from chloride abstraction of **2b** creates in the solvent a strong (unidentified) Brønsted acid which is the catalytically active species. However, when the catalytic reaction was performed in the presence of 20 mol% 2,6-di-*tert*-butylpyridine, the product **5a** was isolated in 42% yield. Thus, it appears to be unlikely that a strong Brønsted acid is the only catalytically active species in solution. Further investigations of these processes are currently underway.

3. Conclusion

In conclusion, we have synthesized and structurally characterized the first chiral at metal Cp phosphoramidite PPh_3 complexes of the general formula CpRu(PPh_3)(L)(Cl) (**2a**–**c**). The X-ray structure analyses showed a slightly distorted octahedral coordination geometry about the ruthenium center. Electrochemical analyses by cyclic voltammetry of the metal complexes CpRu(PPh_3)(L)(Cl) revealed that they undergo reversible oxidation reactions, whereas their corresponding phosphoramidite ligands show irreversible electrochemical behavior. The chloride ligand of complex **2b** can be removed by (Et_3O)(PF_6). The resulting fragment is catalytically active in the Mukaiyama aldol reaction but produced almost no enantiomeric excess.

4. Experimental

4.1. General

Chemicals were treated as follows: diethyl ether, distilled from Na/benzophenone; CH_2Cl_2, distilled from CaH_2, MeOH and $CHCl_3$ used as received. CpRu(PPh_3)$_2$Cl (Strem), (Et_3O)(PF_6), silica (Aldrich), Florisil® (Fisher) and other materials, used as received. "(*R*)-BINOL-*N*,*N*-dimethyl-phosphoramidite" **1a** and "(*R*)-BINOL-*N*,*N*-dibenzyl-phosphoramidite" **1b** were synthesized according to literature procedures [13] as well as "(*R*)-BINOL(8*H*)-*N*,*N*-dibenzyl-phosphoramidite" (**1c**) [14]. All reactions were carried out under nitrogen employing standard Schlenk techniques, and workups were carried out in the air.

NMR spectra were obtained at room temperature on a Bruker Avance 300 MHz or a Varian Unity Plus 300 MHz instrument and referenced to a residual solvent signal; all assignments are tentative. GC/MS spectra were recorded on a Hewlett Packard GC/MS System Model 5988A. Exact masses were obtained on a JEOL MStation [JMS-700] Mass Spectrometer. Melting points are uncorrected and were taken on an Electrothermal 9100 instrument. IR spectra were recorded on a Thermo Nicolet 360 FT-IR spectrometer. Elemental analyses were performed by Atlantic Microlab Inc., Norcross, GA, USA.

4.1. Synthesis of "((R)-BINOL-N,N-dimethyl-phosphoramidite)CpRuCl(PPh_3)" (**2a**)

To a Schlenk flask containing phosphoramidite **1a** (0.400 g, 1.11 mmol) and CpRu(PPh_3)$_2$Cl (0.735 g, 1.01 mmol), $CHCl_3$ (15 mL) was added and the solids dissolved. The orange solution was then heated to reflux for 8 h. Upon cooling, the solvent was removed under vacuum, giving an orange solid. The solid was purified by flash chromatography (2.5 × 17 cm Florisil®, CH_2Cl_2/Et_2O 49:1 v/v) to obtain **2a** as a yellow solid as mixture of diastereomers (5:3, ^{1}H NMR) (0.535 g, 0.650 mmol, 64%), m.p. 202–203 °C dec. (capillary). *Anal.* Calc. for $C_{45}H_{38}ClNO_2P_2Ru$: C, 65.65; H, 4.65. Found: C, 65.27; H, 4.77%.

NMR (δ, $CDCl_3$) ^{1}H 7.86 (d, J_{HH} = 8.6 Hz, 2H, binaphthyl), 7.82 (d, J_{HH} = 4.5 Hz, 0.6H, binaphthyl′), 7.80 (d, J_{HH} = 3.5 Hz, 1H, binaphthyl), 7.77 (d, J_{HH} = 2.9 Hz, 1H, binaphthyl), 7.06 (d, J_{HH} = 8.2 Hz, 0.6H, binaphthyl′) 7.63–7.53 (m, 3H, aromatic), 7.40–7.35 (m, 4H, aromatic), 7.34–7.21 (m, 10H, aromatic), 7.19–7.08 (m, 10H, aromatic), 7.06 (d, J_{HH} = 1.7 Hz, 1.6H, aromatic), 7.03 (d, J_{HH} = 1.6 Hz, 1.6H, aromatic), 7.02–6.95 (m, 7H, aromatic), 4.48 (s, 5H, Cp), 4.39 (s, 3H, Cp′), 2.42 (s, 3H, NCH_3), 2.39 (s, 3H, NCH_3), 2.30 (s, 1.8H, NCH_3), 2.27 (s, 1.8H, NCH_3); ^{13}C{^{1}H} (partial) 82.9 (s, Cp), 81.9 (s, Cp'), 39.04 (s, NCH_3), 38.96 (s, NCH_3), 38.4 (s, NCH'_3), 38.3 (s, NCH'_3); ^{31}P{^{1}H} 177.8 (d, $^2J_{PP}$ = 168.0 Hz, phosphoramidite) 176.0 (d, $^2J_{PP}$ = 160.2 Hz, phosphoramidite′), 48.7 (d, $^2J_{PP}$ = 168.0 Hz, PPh_3), 46.9 (d, $^2J_{PP}$ = 160.2 Hz, PPh'_3).

HRMS calcd for $C_{45}H_{38}{}^{35}ClNO_2P_2{}^{102}Ru$ 823.1109, found 823.1094. MS (FAB): 823 (**2a**$^+$, 95%), 788 ([**2a**–Cl]$^+$, 60%), 526 ([**2a**–PPh_3–Cl]$^+$, 30%), 429 ([CpRuPPh_3]$^+$, 100%). IR (cm^{-1}, neat solid) 3050 (w), 2840 (w), 2796 (w), 1617 (w), 1589 (m), 1463 (m), 1432 (m), 1229 (s).

4.2. Synthesis of "((R)-BINOL-N,N-dibenzyl-phosphoramidite)CpRuCl(PPh_3)" (**2b**)

To a Schlenk flask containing phosphoramidite **1b** (0.299 g, 0.568 mmol) and CpRu(PPh_3)$_2$Cl (0.387 g, 0.533 mmol), $CHCl_3$ (8 mL) was added and the solids dissolved. The orange solution was then heated to reflux for 16 h. Upon cooling, the solvent was removed under vacuum, giving an orange solid. The solid was purified by flash chromatography (2 × 17 cm silica, CH_2Cl_2/diethyl ether 49:1 v/v) to obtain **2b** as an orange solid as a mixture of diastereomers (>8:1, ^{1}H NMR) (0.444 g, 0.455 mmol). The compound was recrystallized from CH_2Cl_2/MeOH to obtain **2b** as a single diastereomer (0.386 g, 0.395 mmol, 74%), m.p. 189–190 °C dec. (capillary). *Anal.* Calc. for $C_{57}H_{46}ClNO_2P_2Ru$: C, 70.18; H, 4.75. Found: C, 69.89; H, 4.72%.

NMR (δ, $CDCl_3$) ^{1}H 8.06 (d, J_{HH} = 4.9 Hz, 1H, binaphthyl), 8.01 (d, J_{HH} = 5.3 Hz, 1H, binaphthyl), 7.74 (d, J_{HH} = 4.9 Hz, 1H, binaphthyl), 7.55 (t, J_{HH} = 4.3 Hz, 1H, binaphthyl), 7.47 (d, J_{HH} = 5.3 Hz, 1H, binaphthyl), 7.42–7.32 (m, 11H, aromatic), 7.31–7.27 (m, 6H, aromatic), 7.15–7.09 (m, 7H, aromatic), 7.08–6.92 (m, 7H, br, aromatic), 6.73 (d, J_{HH} = 5.3 Hz, 1H, binaphthyl), 4.92 (d, $^2J_{HH}$ = 6.8 Hz, 1H, NC*H*H′), 4.89 (d, $^2J_{HH}$ = 6.8 Hz, 1H, NCH*H*′), 4.71 (s, 5H, Cp), 3.83 (d, $^2J_{HH}$ = 6.1 Hz, 1H, NC*H*H′), 3.79 (d, $^2J_{HH}$ = 6.8 Hz, 1H, NCH*H*′); ^{13}C{^{1}H} (500 MHz) 151.1 (t, J_{CP} = 24.1 Hz, aromatic), 149.3 (s, br, aromatic), 139.6 (s, br, aromatic), 137.9 (s, br, aromatic), 137.6 (s, br, aromatic), 135.0 (s, br, aromatic), 133.8 (d, J_{CP} = 16.5 Hz, aromatic), 132.8 (d, J_{CP} = 17.4 Hz, aromatic), 131.5 (s, br, aromatic), 131.1 (s, br, aromatic), 130.6 (d, J_{CP} = 12.0 Hz, aromatic), 130.4 (d, J_{CP} = 12.0 Hz, aromatic), 129.7 (s, br, aromatic), 129.3 (d, J_{CP} = 12.0 Hz, aromatic), 129.1 (d, J_{CP} = 15.3 Hz, aromatic), 128.4 (s, br, aromatic), 128.2 (s, br, aromatic), 127.8 (d, J_{CP} = 16.2 Hz, aromatic), 127.1 (d, J_{CP} = 18.0 Hz, aromatic), 126.9 (s, br, aromatic), 126.7 (s, br, aromatic), 126.5 (t, J_{CP} = 14.5 Hz, aromatic), 125.8 (d, J_{CP} = 14.3 Hz, aromatic), 125.6 (d, J_{CP} = 14.7 Hz, aromatic), 125.5 (d, J_{CP} = 14.7 Hz, aromatic), 125.0 (d, J_{CP} = 14.8 Hz, aromatic), 123.6 (s, aromatic), 123.4 (s, aromatic), 122.8 (s, aromatic), 122.3 (s, aromatic), 121.5 (s, aromatic), 81.6 (d, J = 176 Hz, br, Cp), 51.2 (d, J = 102.3 Hz, br, NCH_2), 50.1 (d, J = 328.5 Hz, br, NCH_2); ^{31}P{^{1}H}

171.8 (d, $^2J_{PP}$ = 152.2 Hz, phosphoramidite), 45.2 (d, $^2J_{PP}$ = 152.2 Hz, PPh_3).

HRMS calcd for $C_{57}H_{46}{}^{35}ClNO_2P_2{}^{102}Ru$ 975.1735, found 975.1702. MS (FAB) 975 (**2b**$^+$, 90%), 940 ([**2b**–Cl]$^+$, 45%), 678 ([**2b**–PPh_3–Cl]$^+$, 92%), 429 ([$CpRuPPh_3$]$^+$, 100%). IR (cm^{-1}, neat solid) 3052 (m), 1617 (w), 1591 (w), 1460 (w), 1432 (m), 1229 (s).

4.3. Synthesis of "((R)-BINOL(8H)-N,N-dibenzylphosphoramidite)CpRuCl(PPh_3)" (**2c**)

To a Schlenk flask containing phosphoramidite **1c** (0.200 g, 0.385 mmol) and $CpRu(PPh_3)_2Cl$ (0.225 g, 0.310 mmol), $CHCl_3$ (8 mL) was added and the solids dissolved. The orange solution was then heated to reflux for 16 h. Upon cooling, the solvent was removed under vacuum, giving an orange solid. The solid was purified by flash chromatography (2 × 10 cm silica, CH_2Cl_2/diethyl ether 49:1 v/v) to obtain **2c** as an orange solid as a mixture of diastereomers (8:1, ^{1}H NMR) (0.181 g, 0.184 mmol). The compound was recrystallized from CH_2Cl_2/MeOH to obtain **2c** as a single diastereomer (0.141 g, 0.143 mmol, 46%), m.p. 218–219 °C dec. (capillary). *Anal.* Calc. for $C_{57}H_{54}ClNO_2P_2Ru$: C, 69.61; H, 5.53. Found: C, 69.54; H, 5.68%.

NMR (δ, $CDCl_3$) ^{1}H 7.37–7.25 (m, 10H, aromatic), 7.24–7.09 (m, 16H, aromatic), 6.80 (d, $^3J_{HH}$ = 8.2 Hz, 1H, binaphthyl), 6.57 (d, $^3J_{HH}$ = 8.2 Hz, 1H, binaphthyl), 6.21 (d, $^3J_{HH}$ = 8.0 Hz, 1H, binaphthyl), 4.91 (d, $^2J_{HH}$ = 10.0 Hz, 1H, NC*H*H′), 4.85 (d, $^2J_{HH}$ = 10.0 Hz, 1H, NCH*H*′), 4.60 (s, 5H, Cp), 3.41 (d, $^2J_{HH}$ = 10.8 Hz, 1H, NC*H*H′), 3.35 (d, $^2J_{HH}$ = 10.8 Hz, 1H, NCH*H*′), 2.96 (t, $^3J_{HH}$ = 6.0 Hz, 2H, CH_2), 2.72–2.38 (m, 4H, $2CH_2$), 2.11–1.95 (m, 2H, CH_2), 1.92–1.71 (m, 3H), 1.70–1.55 (m, 4H, $2CH_2$), 1.40–1.25 (m, 1H); $^{13}C\{^1H\}$ 149.3 (d, J_{CP} = 60.0 Hz, aromatic), 148.6 (d, J_{CP} = 24.0 Hz, aromatic), 139.8 (d, J_{CP} = 7.8 Hz, aromatic), 139.1 (s, aromatic), 138.2 (s, aromatic), 137.8 (s, aromatic), 137.6 (s, aromatic), 134.4 (s, br, aromatic), 133.5 (s, aromatic), 133.4 (s, aromatic), 129.3 (s, aromatic), 129.2 (s, aromatic), 129.0 (s, aromatic), 128.4 (s, aromatic), 128.1 (s, aromatic), 127.7 (s, aromatic), 127.6 (s, aromatic), 127.4 (d, J_{CP} = 36.0 Hz, aromatic), 127.1 (d, J_{CP} = 9.1 Hz, aromatic), 126.9 (s, aromatic), 81.0 (s, Cp), 50.1 (s, NCH_2), 50.0 (s, NCH_2), 29.7 (s, CH_2), 29.2 (s, CH_2), 28.2 (s, CH_2), 27.6 (s, CH_2), 23.1 (s, CH_2), 23.0 (s, CH_2), 22.9 (s, CH_2), 22.8 (s, CH_2); $^{31}P\{^1H\}$ 163.8 (d, $^2J_{PP}$ = 148.5 Hz, phosphoramidite), 46.0 (d, $^2J_{PP}$ = 148.5 Hz, PPh_3).

HRMS calcd for $C_{57}H_{54}{}^{35}ClNO_2P_2{}^{102}Ru$ 983.2361, found 983.2329. MS (FAB): 983 (**2c**$^+$, 45%), 948 ([**2c**–Cl]$^+$, 15%), 686 ([**2c**–PPh_3–Cl]$^+$, 100%), 429 ([$CpRuPPh_3$]$^+$, 95%). IR (cm^{-1}, neat solid) 3052 (m), 3022 (m), 2929 (s), 2858 (m), 1582 (w), 1469 (s), 1433 (s).

4.4. X-ray structure analyses

To obtain crystals of X-ray quality, **2b** was dissolved in THF and layered with hexanes and **2c** was dissolved in $CHCl_3$ and layered with MeOH and both samples stored at −18 °C. X-ray structure data were collected and analyzed as described before [21].

Crystal data and intensity data collection parameters are listed in Table 1. Structure solution and refinement were carried out using the SHELXTL-PLUS software package [22]. The structures were solved by direct methods and refined successfully in the space groups $P2_12_12_1$ and $P2_1$, respectively. Full matrix least-squares refinement was carried out by minimizing $\sum w(F_o^2 - F_c^2)^2$. The non-hydrogen atoms were refined anisotropically to convergence. All hydrogen atoms were calculated in their idealized geometry and were treated using appropriate riding model (AFIX m3). Disorder in the solvent molecule ($CHCl_3$) in case of **2c** and the 2 THF molecules in case of **2b** were resolved with partial occupancy atoms.

Table of calculated and observed structure factors are available in electronic format.

4.5. Cyclic voltammetry

The voltamogramms were recorded with a Princeton Applied Research Parstat 2273 Electrochemical System and analyzed with POWERSUITE 2.58 software. Cells were fitted with a glassy carbon working electrode, and an Ag wire pseudoreference electrode and a platinum wire as auxiliary electrode. All CH_2Cl_2 solutions were 1×10^{-3} M in substrate and 0.05 M in n-$Bu_4N^+ \cdot PF_6^-$ and degassed with argon. All cyclic voltammograms were recorded with a scan rate of 100 mV s^{-1}. Ferrocene was subsequently added, and calibration voltammograms recorded. All potentials are references to the observed $E_{1/2}$ value for the ferrocene/ferrocenium couple. The ambient laboratory temperature was 22 ± 1 °C.

4.6. Catalytic experiments

A batch solution of the activated catalyst was prepared first. Complex **2b** (0.029 g, 0.0297 mmol) and $(Et_3O)(PF_6)$ (0.006 g, 0.0241 mmol) were combined in CH_2Cl_2 (6 mL) under nitrogen and maintained at room temperature for 2 h. A deep orange solution resulted, and 1.5 mL of the solution (equivalent to 0.007 g, 0.007 mmol catalyst **2b**) was added to the silane **3** (0.472 mmol) and the carbonyl compound **4** (0.472 mmol). After 24 h at room temperature, the solvent was removed and the residue purified by column chromatography (1 × 8 cm silica gel, CH_2Cl_2/cyclohexane 2:1 v:v) to obtain **5** as slightly yellow oils.

Acknowledgments

We thank Dr. Keith Stine (University of Missouri – St. Louis) for assistance with the cyclic voltammograms. We thank the University of Missouri – St. Louis (Research Board) for support. Funding from the National Science Foundation for the purchase of the Apex-II diffractometer (MRI, CHE-0420497), the purchase of the NMR spectrometer (CHE-9974801) and the purchase of the mass spectrometer (CHE-9708640) is acknowledged.

Appendix A. Supplementary material

CCDC 694648 and 694647 contain the supplementary crystallographic data for **2b** and **2c**. These data can be obtained free of charge from The Cambridge Crystallographic Data Centre via www.ccdc.cam.ac.uk/data_request/cif. NMR spectra (^{1}H, ^{13}C) for compounds **5a**–**d** (Table 4) as well as spectra for the determination of enantiomeric excesses and the cyclic voltamogramms for compounds **1b**–**c** and **2b**–**c**. Supplementary data associated with this article can be found, in the online version, at doi:10.1016/j.ica.2008.09.003.

References

[1] (a) N. Mršić, L. Lefort, J.A.F. Boogers, A.J. Minnaard, B.L. Feringa, J.G. de Vries, Adv. Synth. Catal. 350 (2008) 1081;
(b) A.J. Minnaard, B.L. Feringa, L. Lefort, J.G. de Vries, Acc. Chem. Res. 40 (2007) 1267;
(c) W. Zhang, X. Zhang, J. Org. Chem. 72 (2007) 1020;
(d) B. Zhao, Z. Wang, K. Ding, Adv. Synth. Catal. 348 (2006) 1049;
(e) M. van den Berg, A.J. Minnaard, R.M. Haak, M. Leeman, E.P. Schudde, A. Meetsma, B.L. Feringa, A.H.M. de Vries, C.E.P. Maljaars, C.E. Willans, D. Hyett, J.A.F. Boogers, H.J.W. Henderickx, J.G. de Vries, Adv. Synth. Catal. 345 (2003) 308;
(f) A.H.M. de Vries, A. Meetsma, B.L. Feringa, Angew. Chem., Int. Ed. Engl. 35 (1996) 2375.
[2] (a) B. Maciá, A. Fernández-Ibáñez, N. Mršić, A.M. Minnaard, B.L. Feringa, Tetrahedron Lett. 49 (2008) 1877;
(b) T. Pfretzschner, L. Kleemann, B. Janza, K. Harms, T. Schrader, Chem. Eur. J. 10 (2004) 6048.
[3] (a) L. Eberhardt, D. Armspach, J. Harrowfield, D. Matt, Chem. Soc. Rev. 37 (2008) 839;
(b) I.D. Kostas, K.A. Vallianatou, J. Holz, A. Börner, Tetrahedron Lett. 49 (2008) 331;
(c) W. Zhang, X. Zhang, Angew. Chem., Int. Ed. 45 (2006) 5515.

[4] (a) S. Shekar, B. Trantow, A. Leitner, J.F. Hartwig, J. Am. Chem. Soc. 128 (2007) 11770;
(b) E. Rauly, C. Claver, O. Pàmies, M. Diéguez, Org. Lett. 9 (2007) 49;
(c) M.D.K. Boele, P.C.J. Kamer, M. Lutz, A.L. Spek, J.G. de Vries, P.W.N.M. van Leeuwen, G.P.F. Strijdonck, Chem. Eur. J. 10 (2004) 6232;
(d) M. Kimura, Y. Uozumi, J. Org. Chem. 72 (2007) 707.
[5] J.F. Jensen, B.Y. Svendsen, T.V. la Cour, H.L. Pedersen, M. Johannsen, J. Am. Chem. Soc. 124 (2002) 4558.
[6] A. Duursma, J.-G. Boiteau, L. Lefort, J.A.F. Boogers, A.H.M. de Vries, J.G. de Vries, A.J. Minnaard, B.L. Feringa, J. Org. Chem. 69 (2004) 8045.
[7] (a) N. Toselli, D. Martin, M. Achard, A. Tenaglia, T. Bürgi, G. Buono, Adv. Synth. Catal. 350 (2008) 280;
(b) B.M. Trost, S.M. Silverman, J.P. Stambuli, J. Am. Chem. Soc. 129 (2007) 12398;
(c) B.M. Trost, N. Cramer, S.M. Silverman, J. Am. Chem. Soc. 129 (2007) 12396;
(d) B.M. Trost, J.P. Stambuli, S.M. Silverman, U. Schwörer, J. Am. Chem. Soc. 128 (2006) 13328.
[8] J.W. Faller, P.P. Fontaine, Organometallics 24 (2005) 4132.
[9] R. Imbos, A.J. Minnaard, B.L. Feringa, Dalton Trans. (2003) 2017.
[10] I.S. Mikhel, H. Rüegger, P. Butti, F. Camponovo, D. Huber, A. Mezzetti, Organometallics 27 (2008) 2937.
[11] D. Huber, P.G. Anil Kumar, P.S. Pregosin, I.S. Mikhel, A. Mezzetti, Helv. Chim. Acta 89 (2006) 1696.
[12] C.A. Mebi, R.P. Nair, B.J. Frost, Organometallics 26 (2007) 429. and literature cited therein.
[13] (a) R. Hulst, N.K. de Vries, B.L. Feringa, Tetrahedron: Asymmetry 5 (1994) 699;
(b) L.A. Arnold, R. Imbos, A. Mandoli, A.H.M. de Vries, R. Naasz, B.L. Feringa, Tetrahedron 56 (2000) 2865;
(c) A. Rimkus, N. Sewald, Org. Lett. 5 (2003) 79.
[14] S. Costin, N.P. Rath, E.B. Bauer, Adv. Synth. Catal. (2008), doi: 10.1002/adsc.200800355.
[15] (a) D. Carmona, C. Vega, N. García, F.J. Lahoz, S. Elipe, L.A. Oro, M.P. Lamata, F. Viguri, R. Borao, Organometallics 25 (2006) 1592;
(b) D. Carmona, F.J. Lahoz, S. Elipe, L.A. Oro, M.P. Lamata, F. Viguri, F. Sánchez, S. Martínez, C. Cativiela, M.P. López-Ram de Víu, Organometallics 21 (2002) 5100;
(c) K. Hiroi, K. Watanabe, Tetrahedron: Asymmetry 13 (2002) 1841.
[16] (a) R.S. Cahn, C. Ingold, V. Prelog, Angew. Chem., Int. Ed. Engl. 5 (1966) 385;
(b) K. Stanley, M.C. Baird, J. Am. Chem. Soc. 97 (1975) 6598.
[17] W.E. Geiger, in: P.T. Kissinger, W.R. Heinemann (Eds.), Laboratory Techniques in Electroanalytical Chemistry, Marcel Dekker, New York, 1996, pp. 684–717.
[18] D. Huber, P.G.A. Kumar, P.S. Pregosin, A. Mezzetti, Organometallics 24 (2005) 5221.
[19] (a) T. Mukaiyama, K. Banno, K. Narasaka, J. Am. Chem. Soc. 96 (1974) 7503;
(b) C. Palomo, M. Oiarbide, J.M. García, Chem. Eur. J. 8 (2002) 37.
[20] T.K. Hollis, B. Bosnich, J. Am. Chem. Soc. 117 (1995) 4570.
[21] S.L. Sedinkin, N.P. Rath, E.B. Bauer, J. Organomet. Chem. 693 (2008) 3081.
[22] G.M. Sheldrick, Acta Crystallogr., Sect. A 64 (2008) 112.